

UDC 621.791.9-023.5

Molochkov D. Post-graduate student, National University Zaporizhzhia Polytechnic, Zaporizhzhia, Ukraine, e-mail: molochkov@zp.edu.ua, ORCID: 0000-0002-9030-5371
Kulykovskiy R. Candidate of Technical Sciences, Associate Professor of the Department of Metal Forming, National University Zaporizhzhia Polytechnic, Zaporizhzhia, Ukraine, e-mail: kulikovski@zp.edu.ua, ORCID: 0000-0001-8781-2113

PULSE DEPOSITION METHOD FOR WIRE AND ARC ADDITIVE MANUFACTURING

Purpose. To reduce the waviness of the side surfaces of wire and arc additive manufactured parts.

Research methods. Two groups of deposited specimens were used. The waviness of the side surfaces was measured from digital images of the cross sections of the specimens. The images were obtained by optical digital scanning. To establish a functional relationship between the geometric parameters of the beads and the main deposition parameters, regression and analysis of variance were performed on the measured data.

Results. It was found that different combinations of the main process parameters resulted in a surface waviness of 1.21 ± 0.23 mm. Based on the results obtained, a pulse deposition method was developed. The implementation of regular pauses reduced the heat input and the time spent by the material in the molten state, which limited its distribution. The proposed method resulted in a significantly lower waviness of 0.47 ± 0.08 mm and a significant improvement in the stability of the resulting surface irregularity.

Scientific novelty. It has been shown for the first time that the waviness of the side surfaces in wire and arc additive manufacturing does not depend on the main deposition parameters, but is related to the nature of the arc-based deposition process. The developed method of pulsed deposition limits the time the metal remains in the molten state, which reduces the waviness of the surfaces by up to 60% and improves the stability of the geometry by three times, reducing the standard deviation to 0.08 mm.

Practical value. Pulsed deposition improves the predictability of the printed geometry by improving the accuracy and quality of the side surfaces. This reduces the required machining allowance, speeds up production, and reduces material waste. In some cases, the predictability of the geometry makes it possible to eliminate post-processing.

Key words: additive manufacturing, 3D printing, WAAM, GMAW, arc welding, waviness, surfaces, heat input, parameter optimization.

Introduction

Modern manufacturing processes are focused on enhancing the functionality and service life of components and tools, which could be achieved using advanced materials with improved characteristics. Despite their high-performance properties, such materials are also costly, making the optimal use of each material a priority in production. The efficiency of materials can be enhanced by adopting cutting-edge additive manufacturing technologies, which allow for the optimization of the ratio of material used to the weight of the finished product, thereby reducing waste and increasing the utilization of material in the final product [1].

The quality of parts produced through additive manufacturing based on arc welding (WAAM), without additional mechanical post-processing, often proves to be unacceptable, as the deviations in the shape of such parts and the geometry of their surfaces significantly impair the accuracy of dimensions and mechanical properties, which must meet the requirements set by designers. At the same time, the use of mechanical cutting processing resolves the issue of surface quality and geometric accuracy, but the removal of excess material added for machining allowance, as well as the use of cutting tools, leads to additional material costs and increases production time.

Eliminating or reducing post-processing can potentially speed up the production of parts that are not demanding in terms of surface quality, as well as reduce their cost. However, the characteristic waviness of surfaces typical for the WAAM method, which negatively affects the strength of the parts and their resistance to cracking, must be considered at the design or production stage [2–4]. Predicting the mechanical characteristics of printed components is complicated by the unstable unevenness of the lateral surfaces in the longitudinal and transverse directions to the layers, which is formed by the peculiarity of metal transfer and bead formation in the WAAM process based on GMAW (Gas Metal Automatic Welding).

Optimization of the bead formation process in metal is a relevant scientific and technical issue, the resolution of which will ensure high-quality geometry of the surfaces of the printed parts, improve the efficiency of material use, and reduce the volume of post-processing.

Analysis of Research and Publications

To ensure acceptable quality of WAAM parts, especially when used without post-processing, it is necessary to optimize the unevenness of the lateral surfaces of the printed parts by controlling the geometric parameters of each individual layer of the product. The main

parameters are the width and height of both individual beads and their combinations. This simplified characterization allows for planning the growth trajectory and segmenting 3D models into separate layers. Unbalanced printing parameters inevitably lead to the formation of welding defects such as pores and lack of fusion, as well as deviations in the shape of the printed part.

WAAM based on GMAW is a complex additive process based on the principles of arc welding with a consumable electrode in a shielded gas environment. Accordingly, the main technological parameters of WAAM can be considered the wire feed speed (WFS) and the travel speed of the torch (TS). Additionally, some studies mention the impact of the interpass surface temperature on the geometric parameters of both individual beads and the printed objects as a whole [5].

Optimization of technological parameters in WAAM is the central theme of many studies aimed at improving productivity, optimizing the geometry of printed parts, and reducing residual stresses caused by the thermal cycles of layer-by-layer growth. These studies indicate that among all technological parameters, the wire feed speed (WFS) and the travel speed of the torch (TS) are key factors that affect the geometric parameters of the beads, the stability of the WAAM process, and the accompanying thermal cycles [5, 6]. In various studies concerning the quality of the geometry of printed parts, the effective wall width (EWW) is often discussed in terms of its relationship with the main technological parameters of WAAM, namely WFS and TS [6–8].

In the context of WAAM, particularly when growing thin-walled parts, the effective wall width (EWW) and the total wall width (TWW) can be considered as one of the criteria for assessing the optimality of the chosen technological parameters. The ratio of TWW/EWW can serve as a criterion for selecting among several combinations of parameters that provide the same size of TWW or EWW. A lower ratio indicates less surface waviness and, therefore, higher material usage efficiency. With the same EWW achieved by different combinations of WFS and TS parameters, the least surface waviness will ensure the smallest TWW/EWW ratio.

Among the main parameters, WFS directly ensures the delivery of a specific volume of filler material to the application site per unit of time. Moreover, WFS is directly related to the magnitude of the welding current, which, in turn, is directly proportional to the amount of heat input [9]. WFS must be balanced with TS to ensure a stable arc burning process and, accordingly, a stable geometry of the deposited layer. TS, along with WFS, provides a certain volume of filler material per unit length of the trajectory, which can significantly affect the width of the weld bead and the overlap of adjacent beads. It is also noted that TS directly influences the heating rate of the base material, as this parameter determines the time the heat source remains on a specific segment of the trajectory. At lower TS values, the heat input and the width of the beads increase, while at higher TS, insufficient fusion between layers and unstable bead shape may occur [7, 8]. Thus, heat input, controlled

by TS and the magnitude of the welding current, as well as WFS, significantly affect the height-to-width ratio of the bead. With an increase in heat input, the height-to-width ratio of the bead decreases, while an increase in WFS causes this ratio to increase. Additionally, as the height of the bead increases, the wetting angle of the surface by the applied bead also increases, whereas an increase in the bead width decreases it. [8–11].

Based on existing research, optimizing WFS and TS is the most effective method to ensure control over the geometry of the beads, maintain process stability, and achieve good surface quality and dimensional accuracy of WAAM parts. [12–14].

Objective of the work

In the context of the identified problem, the main objective of the work is to reduce the waviness of the lateral surfaces of parts manufactured using the WAAM method. To achieve this objective, it is necessary to:

- Experimentally determine the dependence of waviness on the technological parameters WFS and TS;
- Based on the experiment, analyse the bead formation and identify the main causes of the unstable process of metal bead formation;
- Develop a method to reduce the waviness of the lateral surfaces by improving the control of heat input and the deposition of filler metal.

Materials and Methods

The previously determined range of optimal technological parameters for WAAM [15] ensures the stability of individual bead formation in the longitudinal direction of the deposition trajectory. However, to assess the suitability of a particular combination of WFS and TS parameters for use with reduced post-processing, it is necessary to investigate the lateral surfaces of the walls formed during multi-layer growth. For this purpose, based on the previous range, a practical experiment with multi-layer growth of single-pass walls was planned. Four values of WFS and TS parameters from the range defined in the previous section were selected for this. Based on the selected factors, a full factorial experiment with sixteen parameter combinations (Table 1) was conducted, which was used to fabricate sixteen samples

Each sample consisted of ten layers of single-pass beads, each 85 mm in length. The beads of the first layer of all samples were deposited on the surface of a metal plate with the same welding parameters to form the base of the walls. Subsequent beads were deposited with the respective welding parameters, changing the deposition direction every second layer. This growth strategy eliminated the effect of height accumulation at the beginning of the wall and height drop at its end. The contact tip to work distance (CTWD) was maintained at a constant value of 13 mm. The interpass temperature was controlled at $100 \pm 10^\circ\text{C}$ to eliminate the heat accumulation effect, which influences the fluidity of the metal [16, 17].

Table 1 – Design of experiment for determining the relationship of surface quality with WFS and TS

Sample #	WFS, m/min	TS, cm/min
1	2	30
2	4	30
3	6	30
4	8	30
5	2	40
6	4	40
7	6	40
8	8	40
9	2	50
10	4	50
11	6	50
12	8	50
13	2	60
14	4	60
15	6	60
16	8	60

The primary filler material chosen for the experiment was welding wire made of heat-resistant stainless alloy 718 with a diameter of 1.2 mm. This material is popular in the aerospace engine industry and widely used in power generation units. Alloy 718 is well-suited for welding, and thus the WAAM process is not accompanied by defects such as porosity or cracking. Given the chemical composition of the material, the growth was performed in an argon environment with a purity of 99.993%. For the substrate, low-carbon structural steel sheet was chosen, as it has sufficient compatibility with alloy 718 to form a strong metallurgical bond until the growth is completed and testing is conducted.

For sample growth, a Yaskawa Motoman MA1440 welding robot equipped with a Fronius TPS500i welding power source, WF25i and WF60i Robacta Drive wire feeders, and a Fronius MTB 500i WR 22° welding torch was used.

Research Results

Upon completion of sample fabrication, a qualitative assessment of the material deposition process and the longitudinal stability of the bead geometry during multilayer growth was conducted. As expected, sample 4 with the highest WFS/TS ratio lost its shape after the third deposited layer (Fig. 1). The loss of shape was due to a significant excess of metal and the amount of heat input, which, combined with the lowest TS, provided the highest linear energy among the studied samples. This led to an increase in the size of the molten metal pool and its overflow with filler material. The excess material per unit length of the bead resulted in its spilling, manifesting as a wide and uneven bead shape. The other samples demonstrated satisfactory longitudinal stability of bead shape.

The primary parameter for evaluating the geometry quality of the printed parts is the waviness of the lateral surfaces, as defined by ISO 21920-2 (formerly ISO 4287) [18]. The smallest absolute value of waviness (W_t)

indicates stability and consistency of the forming process, ensuring the best possible operational properties and material usage efficiency.

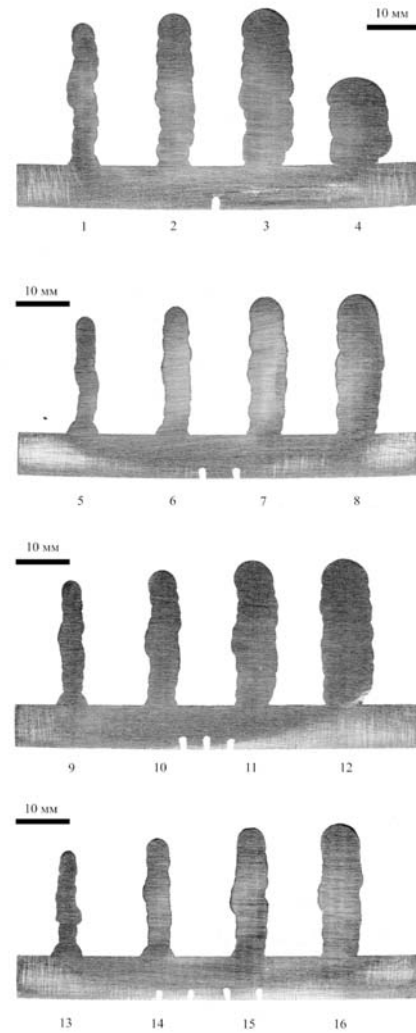


Figure 1. Cross-sections of samples with continuous beads

To assess the cross-sectional shapes of the printed samples, surface maps with the initial profile of each sample were created based on their scanned images (density of 1200 pixels/inch or 47.244 pixels/mm) using ImageJ software. By applying a Gaussian filter according to ISO 16610-21, the waviness profile was separated from the roughness component.

The waviness measurements were taken over a specific evaluation length, which was the full length of the lateral surface profile of each sample, excluding the first and last deposited layers. This exclusion is justified by the fact that the first layer is deposited on a cold substrate, resulting in a smaller width and greater height compared to subsequent layers. Therefore, when studying EWW and the maximum waviness W_t , this could significantly affect the measurement results. For the same reason, the last layer, which has a curved shape, was excluded from the calculations as it could significantly distort the

measurement results. To simplify the analysis, a profile length of 2 mm from the substrate and the surface of the last layer was excluded.

The measurements of TWW and EWW showed a consistent relationship with WFS and TS, similar to what was previously determined [15]. At the same time, the waviness W_t measured based on the profiles of the studied samples was 1.21 ± 0.23 mm. Since WFS and TS collectively determine the linear energy, it is logical to seek a connection between the waviness and linear energy. The Pearson correlation coefficient of 0.68 between the total waviness and linear energy indicates a strong positive linear correlation of the variables. However, despite the correlation coefficient, it is impossible to establish a significant functional relationship between these parameters.

Thus, the experiment with multilayer growth confirmed the adequacy of the previously determined range of WFS and TS parameters, beyond which the stability of bead formation is disrupted, making it impossible to continue the growth process. Since the selected combinations of WFS and TS parameters for the study form walls with a waviness of 1.21 ± 0.23 mm, considering the absence of a functional relationship between the waviness and WAAM technological parameters, the optimality of the latter will be determined by EWW according to the design of individual parts.

The absence of a functional relationship, along with qualitative and quantitative analyses of the sample profiles, indicates that the resulting waviness is caused not so much by a specific combination of technological parameters but by the nature of the process itself, which uses an electric arc as a heat source. The probability of abnormally high waviness is extremely high, especially when using higher values of linear energy. The overflow of the molten metal pool disrupts the stability of the pool shape and the printed elements, affecting the quality of component formation in additive manufacturing and the deposition productivity of WAAM. This is corroborated by other studies, which state that WAAM has potential issues with morphological accuracy due to arc metallurgy mechanisms with complex thermal cycles [19].

Based on the analysis of unsatisfactory combinations of technological parameters, a pulsed material deposition method was proposed to improve the control of bead formation. Pulsed deposition, or material deposition in portions, can provide lower heat input into the part by periodically turning off the arc. Dynamic processes in the molten metal pool can cause disturbances in bead geometry. Bead formation can be particularly unstable with critical combinations of the main WAAM process parameters. Therefore, to limit the flow of molten metal and shorten the lifespan of the molten metal pool, it was proposed to use pulsed delivery of both filler material and energy for melting. Periodic interruptions in the process help control the size of the molten metal pool and limit the metal's spread.

The proposed method involves using discrete portions of metal in the form of deposited points. Each such

portion of deposited material can be described by its diameter D and height H . According to a previous experiment [15], which established the relationship between bead width and height and WAAM technological parameters, the size of the point can be determined by WFS and its deposition time AT (active time) (Fig. 2).

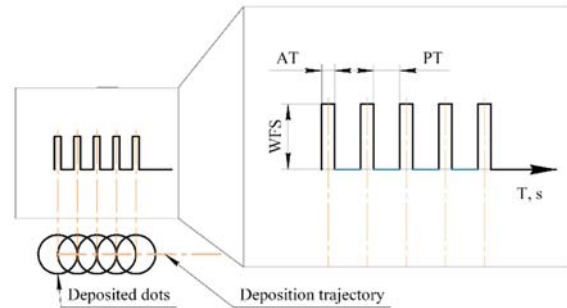


Figure 2. Pulsed deposition diagram

Thus, the formation of a continuous bead, consisting of a chain of individual points, is controlled by the size D of one point, the torch travel speed TS , and the non-deposition time PT (passive time) (Fig. 2). Therefore, the first step in developing the pulsed material deposition method is to establish the dependence of the sizes of individual points on the WFS and AT parameters. Based on the previously determined range of parameters, a 3×3 experiment matrix was constructed to study the size of the portion (point) (Table 2).

Table 2 – Dot size evaluation experiment

Sample #	WFS, m/min	AT, s
1	5	0.15
2	5	0.25
3	5	0.35
4	7	0.15
5	7	0.25
6	7	0.35
7	9	0.15
8	9	0.25
9	9	0.35

WFS of 3 m/min was not used in this experiment, as the previous experiment showed a lack of material in three out of four samples with continuous material deposition. In pulsed deposition, even less material is added per unit of time, so the result will be predictably negative for this WFS with sequential point deposition.

As a result of the full factorial experiment, nine samples of points were obtained, deposited in five layers (Fig. 3). To prevent the effect of heat accumulation on the sample geometry, the interlayer temperature was maintained at up to 100°C . During the experiment, the substrate temperature did not exceed 80°C . The average height of individual points was 1.01 ± 0.16 mm. At the same time, correlation analysis showed a strong positive relationship between the point diameter D and WFS. The Pearson coefficient for this pair of parameters was 0.82. A

significant correlation also exists between the point diameter D and the arc time AT , for which the Pearson coefficient was 0.56. Thus, with the increase of both technological parameters, the diameter of the point also increases (Fig. 4). The normality test showed a normal distribution of the measured D values with a high probability ($p = 0.93$). Through regression analysis, the following dependence was obtained:

$$\sqrt{D} = 1.1914 + 0.09946 \times WFS + 1.348 \times AT. \quad (1)$$

According to the T-test, the WFS parameter has the most significant positive effect on the change in point diameter (Table 3). The Fisher criterion for the regression was 126.75, indicating the significance of the constructed model. Its adequacy is confirmed by the coefficient of determination R^2 of 97 % and a standard error of 0.04 mm.



Figure 3. Multilayer dot samples

Table 3 – ANOVA and regression analysis of the dot diameter model

Parameters	WFS	AT
Coeff.	0.09946	1.348
SE Coeff.	0.00755	0.151
T-Value	13.18	8.93
F-Value	173.69	79.81
P-Value	0.000	0.000

To form continuous beads, a methodology for their combination based on point sizes was developed. For this purpose, the optimal TS speed was selected based on previous experiments. Using the selected TS speed and point diameter D , the passive time PT between points was calculated. The passive time and TS determine the distance from the location where the arc of the previous point is turned off to the location where the arc of the next point is ignited. This distance should not exceed a certain value; otherwise, individual points rather than a continuous bead will be formed. It is assumed that the ignition of the arc for the deposition of the next point should start when the torch has traveled a distance equal to the radius of the previous point (Fig. 5). PT can be calculated using a simple formula:

$$PT = \frac{R}{TS}, \quad (2)$$

where PT – is the passive time, s; R – is the radius of the deposited point, mm; TS – is the travel speed of the torch, mm/s.

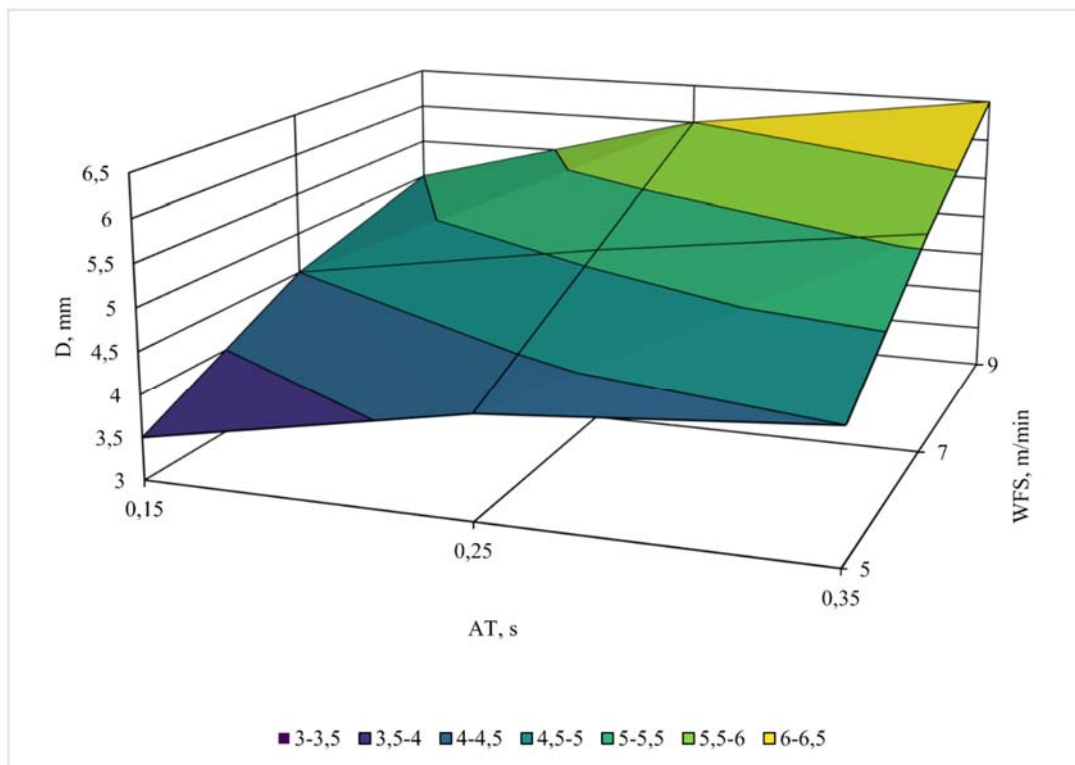


Figure 4. Dependence of deposited dot diameter on WFS and arc time

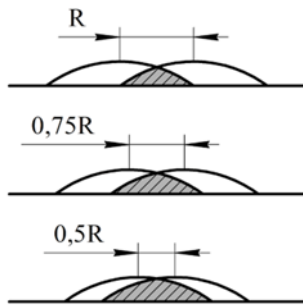


Figure 5. Dot by dot bead formation by pulse deposition

To investigate the possibility of forming continuous beads from individual points, the diameter measurement results were divided into three groups by size ± 0.25 mm. Each group has several parameter combinations that provide similarly sized points. Heat input analysis shows that a combination with higher WFS and lower AT provides less heat input, making it more preferable for application. Additionally, to study the effect of point density on surface irregularity, 75 % and 50 % of the calculated PT were used. Given that three variable parameters were selected for bead formation, the experimental design was developed using the Taguchi method, which, unlike a factorial experiment for testing all combinations, uses an orthogonal array for efficient parameter combination testing (Table 4).

Table 4 – Design of experiment for pulse deposition

PT, s	D, mm	TS, cm/min
t	D1	30
t	D2	40
t	D3	50
0.75t	D1	40
0.75t	D2	50
0.75t	D3	30
0.5t	D1	50
0.5t	D2	30
0.5t	D3	40

Using the selected parameter combinations, nine samples were printed, each consisting of 14 layers (Fig. 6). The first layer was deposited with the same regime parameters to form subsequent layers, so the first layer was not considered in further analysis. The temperature of the samples between layers did not exceed 100 °C. The obtained samples demonstrate significant improvement in geometric stability and reduction in waviness. Measurements showed that the average value of total waviness W_t for all samples decreased to 0.47 mm with a standard deviation of 0.08 mm.

Thus, the proposed pulsed material deposition method reduces waviness from 1.21 mm to 0.47 mm, which is an average reduction of 61 % compared to the waviness formed by traditional continuous material deposition. Additionally, the reduction in the standard error

from 0.23 mm to 0.08 mm, almost three times, indicates a substantial improvement in the uniformity of the lateral surfaces.

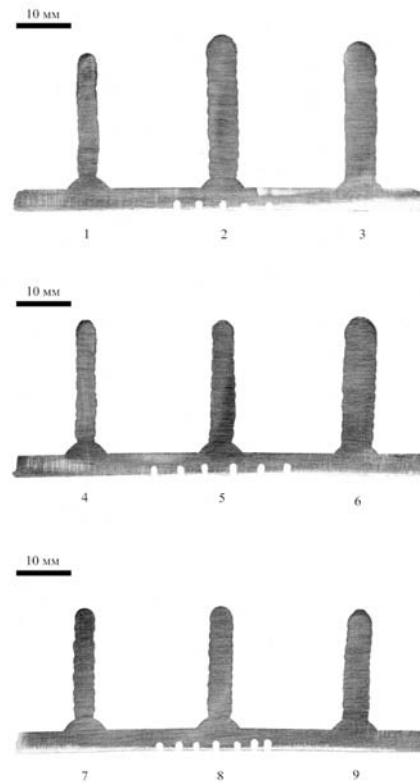


Figure 6. Cross-sections of samples with pulse deposited beads

Comparison of samples with continuous and pulsed material deposition shows that at similar EWW values (e.g., 5.11 mm for sample #2 with continuous deposition and 5.37 mm for sample #6 with pulsed deposition), the TWV/EWW ratio is 1.5 and 1.17, respectively. Thus, reducing waviness improves material usage efficiency. The linear energy during the growth of sample #2 was 380 J/mm. In sample #6, the linear energy was reduced to 272 J/mm due to the introduction of periodic energy delivery interruptions.

Taguchi method analysis established that passive time PT has the greatest effect on the waviness W_t (Fig. 7). The travel speed of the torch TS also shows a significant effect, while the point diameter has almost no impact on waviness. According to the analysis, the smallest waviness is achieved with shorter passive time PT and lower TS. Given that reduced pause time and decreased torch travel speed provide the highest linear energy for given WFS and AT, it can be concluded that the unevenness of the lateral surfaces primarily depends on the size and stability of the molten metal pool. By limiting the time of the deposited metal remaining in the molten state, the quality of the surfaces was improved.

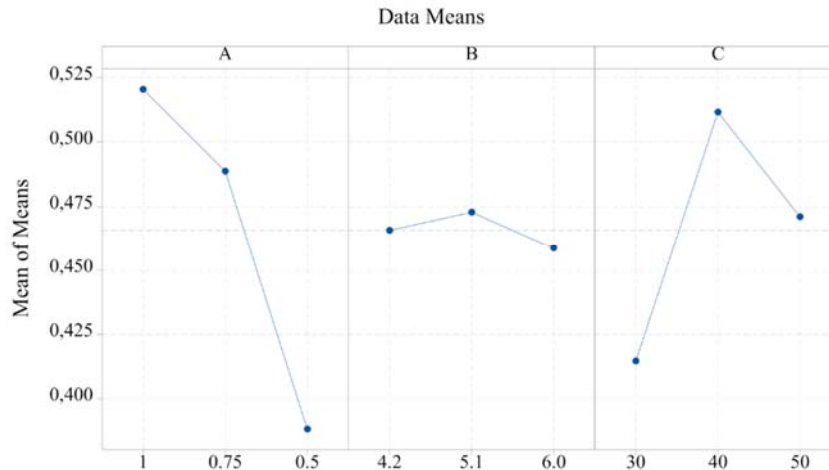


Figure 7. Main Effects Plot for Mean Values of PT (A), D (B) and WFS (C)

Conclusions

As a result of the experiments conducted, it was determined that the selected combinations of WFS and TS parameters from the previously identified range of optimal parameters provide an average surface waviness of 1.21 mm with a standard deviation of 0.23 mm. Thus, it was confirmed that the waviness of WAAM part surfaces is primarily caused by the nature of the arc material deposition process rather than the main technological parameters.

Based on the analysis, a method was proposed and developed to enhance the control of bead formation and reduce surface irregularities by introducing pulsed material deposition and energy delivery for melting the filler material. Deposition with periodic interruptions allowed for a reduction in heat input and the duration of the material in the molten state, thereby limiting its spread. The proposed method provides a waviness of 0.47 ± 0.08 mm, indicating not only a reduction in waviness but also a significant improvement in the repeatability or stability of the formed surface irregularities. At the same time, the introduction of periodic interruptions reduces the linear volume of metal, thus decreasing the production process efficiency.

It was determined that at equal EWW values, the proposed pulsed material deposition method provides a lower TWW/EWW ratio compared to traditional continuous deposition. Reducing this ratio means improved material utilization efficiency, stability of bead formation, and predictability of geometric parameters of both individual beads and printed elements as a whole.

References

1. Cunningham C. R., Wikshåland S., Xu F., Kemakolam N., Shokrani A., Dhokia V., Newman S. T. (2017). Cost Modelling and Sensitivity Analysis of Wire and Arc Additive Manufacturing. *Procedia Manufacturing*, 11, 650–657. doi:10.1016/j.promfg.2017.07.163
2. Lockett H., Ding J., Williams S., Martina F. (2017). Design for Wire + Arc Additive Manufacture:

design rules and build orientation selection. *Journal of Engineering Design*, 28, 7–9, 568–598. doi:10.1080/09544828.2017.1365826

3. Molochkov D., Kulykovskiy R., Brykov M., Hesse O. (2013). The Influence of Surface Irregularities on the Mechanical Properties of Thin-Walled Wire and Arc Additively Manufactured Parts. *Journal of Engineering Sciences* 6 10, 26 A10–A17. doi:10.21272/jes.2023.10(2).a2

4. Peng D., Ang A. S. M., Michelson A., Champagne V., Birt A., Jones R. (2022). Analysis of the Effect of Machining of the Surfaces of WAAM 18Ni 250 Maraging Steel Specimens on Their Durability. *Materials*, 15, 24, 8890. doi:10.3390/ma15248890

5. Teixeira F. R., Scotti F. M., Jorge V. L., Scotti A. (2023). Combined effect of the interlayer temperature with travel speed on features of thin wall WAAM under two cooling approaches. *The International Journal of Advanced Manufacturing Technology* 6 126, 1–26 273–289. doi:10.1007/s00170-023-11105-w

6. Le V. T., Doan Q. T., Mai D. S., Bui M. C., Tran H. S., Tran X. Van, Nguyen V. A. (2022). Prediction and optimization of processing parameters in wire and arc-based additively manufacturing of 316L stainless steel. *Journal of the Brazilian Society of Mechanical Sciences and Engineering*, 44, 9, 394. doi:10.1007/s40430-022-03698-2

7. Dahat S., Hurtig K., Andersson J., Scotti A. (2020). A Methodology to Parameterize Wire + Arc Additive Manufacturing: A Case Study for Wall Quality Analysis. *Journal of Manufacturing and Materials Processing*, 4, 1, 14. doi:10.3390/jmmp4010014

8. Manjhi S. K., Sekar P., Bontha S., Balan A. S. S. (2023). Effect of CMT-WAAM Process Parameters on Bead Geometry, Microstructure and Mechanical Properties of AZ31 Mg Alloy. *Journal of Materials Engineering and Performance*. doi:10.1007/s11665-023-08498-w.

9. Adak D. K., Mukherjee M., Pal T. K. (2015). Development of a Direct Correlation of Bead Geometry, Grain Size and HAZ Width with the GMAW Process

Parameters on Bead-on-plate Welds of Mild Steel. Transactions of the Indian Institute of Metals, 68, 5, 839–849. doi:10.1007/s12666-015-0518-8

10. Rosli N. (2020). Influence of Process Parameter on the Height Deviation of Weld Bead in Wire Arc Additive Manufacturing, 10, 3, 1165–1176. doi:10.24247/ijmperdjun2020101

11. Lam T. F., Xiong Y., Dharmawan A. G., Foong S., Soh G. S. (2020). Adaptive process control implementation of wire arc additive manufacturing for thin-walled components with overhang features. International Journal of Advanced Manufacturing Technology, 108, 4, 1061–1071. doi:10.1007/s00170-019-04737-4

12. Baier D., Wolf F., Weckenmann T., Lehmann M., Zaeh M. F. (2022). Thermal process monitoring and control for a near-net-shape Wire and Arc Additive Manufacturing. Production Engineering, 16, 6, 811–822. doi:10.1007/s11740-022-01138-7

13. Silva L. J. da, Teixeira F. R., Araújo D. B., Reis R. P., Scotti A. (2021). Work Envelope Expansion and Parametric Optimization in WAAM with Relative Density and Surface Aspect as Quality Constraints: The Case of Al5Mg Thin Walls with Active Cooling. Journal of Manufacturing and Materials Processing, 5, 2, 40. doi:10.3390/jmmp5020040

14. Thien A., Saldana C., Kurfess T. (2022). The effect of WAAM process parameters on process conditions and production metrics in the fabrication of single-pass

multi-layer wall artifacts. The International Journal of Advanced Manufacturing Technology, 119, 1–2, 531–547. doi:10.1007/s00170-021-08266-x

15. Molochkov D., Kulykovskiy P., Furmanova N. (2021). Визначення оптимальних параметрів процесу ваам на основі технології cmt з використанням низьковуглецевої нелегованої сталі. Innovative Materials and Technologies in Metallurgy and Mechanical Engineering, 1, 62–68. doi:10.15588/1607-6885-2021-1-9

16. Wu B., Ding D., Pan Z., Cuiuri D., Li H., Han J., Fei Z. (2017). Effects of heat accumulation on the arc characteristics and metal transfer behavior in Wire Arc Additive Manufacturing of Ti6Al4V. Journal of Materials Processing Technology, 250, 304–312. doi:10.1016/j.jmatprotec.2017.07.037

17. Montecchi F., Venturini G., Grossi N., Scippa A., Campatelli G. (2018). Idle time selection for wire-arc additive manufacturing: A finite element-based technique. Additive Manufacturing, 21, 479–486. doi:10.1016/j.addma.2018.01.007

18. International Organization for Standardization (ISO) ISO 21920-2:2021 Geometrical product specifications (GPS) – Surface texture: Profile Part 2: Terms, definitions and surface texture parameters. 2021.

19. Chen X., Kong F., Fu Y., Zhao X., Li R., Wang G., Zhang H. (2021). A review on wire-arc additive manufacturing: typical defects, detection approaches, and multisensor data fusion-based model. The International Journal of Advanced Manufacturing Technology, 117, 3–4, 707–727. doi:10.1007/s00170-021-07807-8

Received 03.04.2024

МЕТОД ІМПУЛЬСНОГО НАНЕСЕННЯ МАТЕРІАЛУ ПРИ АДИТИВНОМУ ВИРОБНИЦТВІ НА ОСНОВІ ЕЛЕКТРОДУГОВОГО ЗВАРЮВАННЯ

Молочков Д. Є. аспірант Національного університету «Запорізька політехніка», м. Запоріжжя, Україна, e-mail: molochkov@zpu.edu.ua, ORCID: 0000-0002-9030-5371

Куликовський Р. А. канд. техн. наук, доцент, доцент кафедри обробки металів тиском Національного університету «Запорізька політехніка», м. Запоріжжя, Україна, e-mail: kulikovski@zpu.edu.ua, ORCID: 0000-0001-8781-2113

Мета роботи. Зменшення хвилястості бокових поверхонь деталей, які виготовляються методом адитивного виробництва на основі електродугового зварювання.

Методи дослідження. Використано дві групи зразків, виготовлених методом адитивного виробництва на основі електродугового зварювання. Хвилястість бокових поверхонь вимірювалась на основі цифрових зображень поперечних перерізів зразків. Зображення отримано шляхом оптично-цифрового сканування. Для встановлення функціонального зв'язку між геометричними параметрами валків і технологічними параметрами процесу виконувався регресійний та дисперсійний аналізи вимірних даних.

Отримані результати. Визначено, що різні комбінації основних технологічних параметрів забезпечують хвилястість поверхонь $1,21 \pm 0,23$ мм. Виходячи з отриманих результатів було розроблено метод імпульсного нанесення матеріалу. Впровадження періодичних переривань дозволило зменшити тепловнесення і час перебування матеріалу в розплавленому стані, що обмежило його розтікання. Запропонований метод забезпечив значно меншу хвилястість $0,47 \pm 0,08$ мм і значне покращення стабільності утвореної нерівномірності поверхонь.

Наукова новизна. Вперше показано, що хвилястість бокових поверхонь при адитивному виробництві на основі електродугового зварювання не залежить від основних технологічних параметрів виробництва, а пов'язана саме з природою процесу нанесення розплавленого металу в цьому методі. Розроблений метод імпульсного нанесення матеріалу обмежує час перебування металу в розплавленому стані, чим досягається

зменшення хвилястості поверхонь на величину до 60 % і покращення стабільності геометрії в три рази, за рахунок зменшення стандартного відхилення до 0,08 мм.

Практична цінність. Імпульсний метод формоутворення покращує передбачуваність вироцуюваної геометрії за рахунок покращення точності та якості бокових поверхонь. Це дозволяє зменшити величину припуску на обробку і пришвидшити виробництво, а також скоротити відходи. В окремих випадках передбачуваність геометрії дозволяє відмовитись від пост-обробки.

Ключові слова: адитивне виробництво, 3Д-друк, WAAM, GMAW, електродугове зварювання, хвилястість, поверхні, тепловнесення, оптимізація параметрів.

Список літератури

1. Cost Modelling and Sensitivity Analysis of Wire and Arc Additive Manufacturing Cunningham C. R., Wikshåland S., Xu F., Kemakolam N. et al. // *Procedia Manufacturing*. – 2017. – Iss. 11, N June 2017. – P. 650–657. doi:10.1016/j.promfg.2017.07.163.
2. Design for Wire + Arc Additive Manufacture: design rules and build orientation selection / Lockett H., Ding J., Williams S., Martina F. // *Journal of Engineering Design*. – 2017. – Iss. 28, N 7–9. – P. 568–598. doi:10.1080/09544828.2017.1365826
3. The Influence of Surface Irregularities on the Mechanical Properties of Thin-Walled Wire and Arc Additively Manufactured Parts / Molochkov D., Kulykovskiy R., Brykov M., Hesse O. // *Journal of Engineering Sciences*. – 2023. – Iss. 10, N 2. – P. A10–A17. doi:10.21272/jes.2023.10(2).a2
4. Analysis of the Effect of Machining of the Surfaces of WAAM 18Ni 250 Maraging Steel Specimens on Their Durability / Peng D., Ang A. S. M., Michelson A. et al. // *Materials*. – 2022. – Iss. 15, N 24. – 8890 p. doi:10.3390/ma15248890
5. Combined effect of the interlayer temperature with travel speed on features of thin wall WAAM under two cooling approaches / Teixeira F. R., Scotti F. M., Jorge V. L., Scotti A. // *The International Journal of Advanced Manufacturing Technology*. – 2023. – Iss. 126, N 1–2. – P. 273–289. doi:10.1007/s00170-023-11105-w
6. Prediction and optimization of processing parameters in wire and arc-based additively manufacturing of 316L stainless steel / Le V. T., Doan Q. T., Mai D. S. et al. // *Journal of the Brazilian Society of Mechanical Sciences and Engineering*. – 2022. – Iss. 44, – N 9. – P. 394. doi:10.1007/s40430-022-03698-2
7. A Methodology to Parameterize Wire + Arc Additive Manufacturing: A Case Study for Wall Quality Analysis / Dahat S., Hurtig K., Andersson J., Scotti A. // *Journal of Manufacturing and Materials Processing*. – 2020. – Iss. 4, N 1. – 14 p. doi:10.3390/jmmp4010014
8. Effect of CMT-WAAM Process Parameters on Bead Geometry, Microstructure and Mechanical Properties of AZ31 Mg Alloy / Manjhi S. K., Sekar P., Bontha S., Balan A. S. S. // *Journal of Materials Engineering and Performance*. – 2023. doi:10.1007/s11665-023-08498-w
9. Development of a Direct Correlation of Bead Geometry, Grain Size and HAZ Width with the GMAW Process Parameters on Bead-on-plate Welds of Mild Steel / Adak D. K., Mukherjee M., Pal T. K. // *Transactions of the Indian Institute of Metals*. – 2015. – Iss. 68, N 5. – P. 839–849. doi:10.1007/s12666-015-0518-8
10. Rosli N. Influence of Process Parameter on the Height Deviation of Weld Bead in Wire / Rosli N. // *Arc Additive Manufacturing*. – 2020. – Iss. 10, N 3. – P. 1165–1176. doi:10.24247/ijmperdjun2020101
11. Adaptive process control implementation of wire arc additive manufacturing for thin-walled components with overhang features / Lam T. F., Xiong Y., Dharmawan A. G. et al. // *International Journal of Advanced Manufacturing Technology*. – 2020. – Iss. 108, N 4. – P. 1061–1071. doi:10.1007/s00170-019-04737-4
12. Thermal process monitoring and control for a near-net-shape Wire and Arc Additive Manufacturing / Baier D., Wolf F., Weckenmann T. et al. // *Production Engineering*. – 2022. – Iss. 16, N 6. – P. 811–822. doi:10.1007/s11740-022-01138-7
13. Work Envelope Expansion and Parametric Optimization in WAAM with Relative Density and Surface Aspect as Quality Constraints: The Case of Al5Mg Thin Walls with Active Cooling / Silva L. J. da, Teixeira F. R., Araújo D. B. et al. // *Journal of Manufacturing and Materials Processing*. – 2021. – Iss. 5, N 2. – 40 p. doi:10.3390/jmmp5020040
14. Thien A. The effect of WAAM process parameters on process conditions and production metrics in the fabrication of single-pass multi-layer wall artifacts / Thien A., Saldana C., Kurfess T. // *The International Journal of Advanced Manufacturing Technology*. – 2022. – Iss. 119, N 1–2. – P. 531–547. doi:10.1007/s00170-021-08266-x
15. Molochkov D. Визначення оптимальних параметрів процесу waam на основі технології cmt з використанням низьковуглецевої нелегованої сталі / Molochkov D., Kulykovskiy P., Furmanova N. // *Innovative Materials and Technologies in Metallurgy and Mechanical Engineering*. – 2021. – N 1. – P. 62–68. doi:10.15588/1607-6885-2021-1-9
16. Effects of heat accumulation on the arc characteristics and metal transfer behavior in Wire Arc Additive Manufacturing of Ti6Al4V / Wu B., Ding D., Pan Z. et al. // *Journal of Materials Processing Technology*. – 2017. – Iss. 250, N August. – P. 304–312. doi:10.1016/j.jmatprotec.2017.07.037
17. Idle time selection for wire-arc additive manufacturing: A finite element-based technique / Montevicchi F., Venturini G., Grossi N. et al. // *Additive Manufacturing*. – 2018. – Iss. 21, N January. – P. 479–486. doi:10.1016/j.addma.2018.01.007
18. International Organization for Standardization (ISO) ISO 21920-2:2021 Geometrical product specifications (GPS) – Surface texture: Profile Part 2: Terms, definitions and surface texture parameters. – 2021.
19. A review on wire-arc additive manufacturing: typical defects, detection approaches, and multisensor data fusion-based model / Chen X., Kong F., Fu Y. et al. // *The International Journal of Advanced Manufacturing Technology*. 2021. – Iss. 117, N 3–4. – P. 707–727. doi:10.1007/s00170-021-07807-8